Int. J. Solids Structures Vol. 20, No. 4, pp. 395 410, 1984
Printed in Great Britain.

0020-7683/84 $3.00 + .00
Pergamon Press Ltd.

MODE III AND MIXED MODE I–II CRACK KINKING UNDER STRESS-WAVE LOADING

J. D. ACHENBACH and M. K. KUO
Department of Civil Engineering, Northwestern University, Evanston, IL 60201, U.S.A.

and

J. P. DEMPSEY
Clarkson College of Technology, Potsdam, NY 13676, U.S.A.

(*Received* 15 *December* 1982; *in revised form* 26 *May* 1983)

Abstract—A stress jump is incident on a line crack in an elastic solid. At the instant that the crack tip is struck, the crack starts to propagate with a constant velocity c_F in the forward direction, but under an angle $\kappa\pi$ with the plane of the original crack. In the time interval before signals from the other crack tip arrive, approximate expressions have been obtained for the elastodynamic stress intensity factors of the kinked crack. The approximation is based on the assumption that the near-tip field for a kinked crack can be approximated by the field for a crack propagating in its own plane, provided that the new crack faces are subjected to appropriate surface tractions. For the Mode-III case the approximation of the elasto-dynamic stress intensity factor for the kinked crack can be checked by comparisons with exact results. The range of kinking angles and crack-tip speeds for which the approximation gives good results turns out to be surprisingly large. For the Mixed Mode I–II case comparisons with numerical results have been carried out, and satisfactory agreement has been obtained. The elastodynamic stress intensity factors have been used to compute the corresponding fluxes of energy into the propagating crack tip. For a specified angle of incidence the energy flux into the crack tip shows a distinct maximum at a specified combination of crack-kinking angle and crack-tip speed.

INTRODUCTION

When a stress pulse strikes a crack, the crack may be induced to propagate, but not necessarily in it's own plane. In earlier papers, see, e.g.[1], it has been attempted to explain kinking of a crack at finite kinking angles. In the present paper we reconsider the two-dimensional configuration of an initially stationary semi-infinite crack which kinks under an angle $\kappa\pi$ with it's original plane. We discuss earlier results for Mode III, and we propose a way to approximate the elastodynamic stress intensity factors for the Mixed Mode I–II case.

The tip of the kinked crack is assumed to propagate at a constant velocity c_F, and kinking is initiated at an angle $\kappa\pi$ at the instant that an incident stress wave first strikes the original crack tip. These two assumptions render the solution self-similar. Three cases are considered corresponding to incidence of either an anti-plane transverse wave, an in-plane transverse wave or a longitudinal wave. The elastodynamic stress intensity factors have been computed as functions of the crack tip speed, c_F, the kinking angle, $\kappa\pi$, and the angle of wave incidence $\alpha\pi$. For a given angle of incidence, the elastodynamic stress intensity factors have been used to compute the corresponding energy fluxes into the propagating crack tip.

Mode-III problems of the kind formulated in this paper can be solved rigorously. For a bifurcating crack two special cases were solved in [2]. Corrected results for Mode-III kinking under an arbitrary angle were given in [3]. The corresponding mixed Mode I–II problems have, however, as yet eluded a rigorous analytical solution. A numerical approach both for the Mode-III and the mixed Mode I–II cases has recently been given by Burgers[4, 5].

For a kinked crack geometry the total field can be considered as the superposition of the field generated by diffraction of the incident wave by a stationary semi-infinite crack and the solution to a superposition problem. The problem for the stationary crack can be analyzed by the use of integral transforms together with an application of the

Wiener–Hopf technique and the Cagniard-de Hoop method. A detailed description of the approach can be found in Ref. [6]. The superposition problem concerns an initially quiescent solid which contains a semi-infinite crack. At time $t = 0$ a branch emanates from the crack tip, and at the same time the new crack faces are subjected to crack-face tractions which are opposite in sign to the stresses computed from the stationary crack problems. The superposition of the fields from the stationary crack problem and the superposition problem renders the faces of crack–kink free of tractions. The singular stresses at the new crack tip equal those from the superposition problem.

For the mixed Mode I–II problems we propose a simple approximation to the solution of the superposition problem. The approximation is based on an observation from the exact Mode-III solution of the analogous superposition problem, that for an important range of kinking angles the elastodynamic stress intensity factor of the kinked crack is affected more by the dependence on κ of the loading on the new crack faces than by the wedge geometry at the original crack tip. This observation then suggests that in first approximation we may ignore the wedge geometry altogether, and we may compute elastodynamic stress intensity factors by considering a crack propagating in its own plane but where the new crack faces are subjected to tractions corresponding to the kinking crack.

For the Mode-III case the approximation of the elastodynamic stress intensity factor for the kinked crack can be checked by comparisons with exact results given by Dempsey *et al.*[3]. The range of kinking angles $\kappa\pi$ for which the approximation gives good results turns out to be surprisingly large. For the mixed Mode I–II case comparisons with the numerical results of Ref. [5] have been carried out, and satisfactory agreement has been obtained. No rigorous mathematical proof of the approximation's validity is given in this paper. It is, however, to be expected that the results correspond to the first order terms in a perturbation procedure for small kinking angle.

The results of this paper suggest that the approximation could be used to analyze crack kinking at gradually increasing angles and at time-varying crack tip speeds. Solutions for crack propagation in the plane of the crack at varying velocity and with arbitrary crack-face loading can be found in the literature; these solutions have been reviewed by Achenbach[7] and Freund[8].

FORMULATION OF THE CRACK KINKING PROBLEM

The incident wave strikes the crack tip at $t = 0$, at which time the crack starts to propagate at a constant velocity c_F, under an angle $\kappa\pi$ with the plane of the crack, thus producing a kinked crack. We concern ourselves with the cases of $c_F < c_T$ for Mode III crack propagation and $c_F < c_R$ for mixed Mode I–II crack propagation, where c_T and c_R are the velocities of transverse waves and Rayleigh surface waves, respectively.

Mode-III crack kinking (incident TH-wave)

We first consider that the incident stress wave is of the form

$$\sigma^{in}_{y'z} = \sigma_0 H(\tau_T), \tag{1}$$

where

$$\tau_T = t + (x/c_T)\sin\alpha\pi - (y/c_T)\cos\alpha\pi = t + (r/c_T)\sin(\alpha\pi - \theta), \tag{2}$$

and α, r and θ are defined in Fig. 1. For diffraction of a step-stress wave by a stationay semi-infinite crack the stress fields depend on r/t and θ, rather than on r, θ and t separately. We find for $r < c_T t$:

$$\sigma^{sl}_{\theta z} = \sigma^{in}_{\theta z} + \sigma^{sc}_{\theta z} \tag{3a}$$

where

$$\sigma^{in}_{\theta z} = \sigma_0 \cos(\alpha\pi - \theta) \tag{3b}$$

$$\sigma^{sc}_{\theta z} = -\Sigma_{xz}\sin|\theta| + \Sigma_{yz}\cos\theta \tag{3c}$$

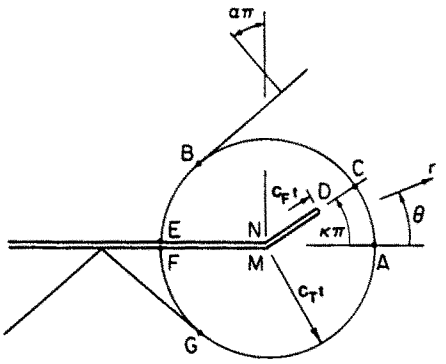

Fig. 1. Geometry of wavefronts for a kinking crack, for an incident horizontally polarized transverse wave; $\alpha\pi$ = angle of incidence, $\kappa\pi$ is kinking angle, c_T = crack-tip speed.

In (3c)

$$\Sigma_{xz} = -\sigma_0 \cos(\alpha\pi) \int_{r/t}^{c_T} \frac{1}{v^2} \Lambda_{xz}(v, \theta)\, dv \tag{4a}$$

$$\Sigma_{yz} = -\sigma_0 \cos(\alpha\pi) \int_{r/t}^{c_T} \frac{1}{v^2} \Lambda_{yz}(v, \theta)\, dv \tag{4b}$$

where

$$\Lambda_{xz}(v, \theta) = \frac{1}{\pi s_T^{1/2}(1 + \sin \alpha\pi)^{1/2}} \operatorname{Im}\left[\frac{\xi_T \cdot d\xi_T/d(1/v)}{(s_T - \xi_T)^{1/2}(\xi_T - s_T \sin \alpha\pi)}\right] \tag{5a}$$

$$\Lambda_{yz}(v, \theta) = \frac{-1}{\pi s_T^{1/2}(1 + \sin \alpha\pi)^{1/2}} \operatorname{Im}\left[\frac{(s_T + \xi_T)^{1/2} \cdot d\xi_T/d(1/v)}{(\xi_T - s_T \sin \alpha\pi)}\right] \tag{5b}$$

and

$$\xi_T(v, \theta) = -\frac{1}{v} \cos\theta + i \sin|\theta| \left[\left(\frac{1}{v}\right)^2 - s_T^2\right]^{1/2}. \tag{6}$$

Here $s_T = 1/c_T$ is the slowness of the transverse wave. The branch cuts have been taken as along the $\operatorname{Re}(\xi_T)$ axis from $\xi_T \to -\infty$ to $\xi_T = -s_T$ and $\xi_T = s_T$ to $\xi_T \to \infty$.

For the superposition problem, the conditions on the crack faces are:

$$\theta = \pm\pi, \quad r > 0: \qquad \sigma_{\theta z} = 0 \tag{7}$$

$$\theta = \kappa\pi \pm 0, \quad 0 < r < c_T t: \qquad \sigma_{\theta z} = -\sigma_{\theta z}^{st}(r/t, \kappa\pi). \tag{8}$$

The fields for horizontally polarized transverse motions only are governed by:

$$\nabla^2 u_z = \frac{1}{c_T^2} \ddot{u}_z, \tag{9}$$

where $u_z(r, \theta, t)$ is the out-of plane displacement, $\dot{(\cdot)} = \partial/\partial t$ and ∇^2 is the two-dimensional Laplacian.

Mixed Mode I–II crack kinking (incident L*-wave and/or* TV*-wave)*

A complete statement of the equations which govern the elasto-dynamic fields is given in Ref. [6]. In the usual manner the displacement components are expressed in terms of

displacement potentials by:

$$u_x = \frac{\partial \phi}{\partial x} + \frac{\partial \psi}{\partial y}, \quad \text{and} \quad u_y = \frac{\partial \phi}{\partial y} - \frac{\partial \psi}{\partial x}, \tag{10a, b}$$

where $\phi(x, y, t)$ and $\psi(x, y, t)$ satisfy uncoupled wave equations:

$$\nabla^2 \phi = \frac{1}{c_L^2} \ddot{\phi}, \qquad c_L^2 = \frac{\lambda + 2\mu}{\rho}; \tag{11a, b}$$

$$\nabla^2 \psi = \frac{1}{c_T^2} \ddot{\psi}, \qquad c_T^2 = \frac{\mu}{\rho}. \tag{12a, b}$$

First, the incident wave is taken as a longitudinal (tension) wave of the form:

$$\sigma_y^{in} = \sigma_0 H(\tau_L), \qquad \epsilon_{x'} \equiv 0 \tag{13}$$

where

$$\tau_L = t + (x/c_L) \sin \alpha\pi - (y/c_L) \cos \alpha\pi = t + (r/c_L) \sin (\alpha\pi - \theta). \tag{14}$$

The stress components σ_θ^{st} and $\sigma_{\theta r}^{st}$ corresponding to the stationary crack problem are, for $r < c_L t$,

$$\sigma_\theta^{st} = \sigma_\theta^{in} + \sigma_\theta^{sc}, \quad \sigma_{\theta r}^{st} = \sigma_{\theta r}^{in} + \sigma_{\theta r}^{sc} \tag{15a, b}$$

where

$$\sigma_\theta^{in} = \sigma_0[1 - 2(c_T/c_L)^2 \sin^2(\alpha\pi - \theta)] \tag{16a}$$

$$\sigma_{\theta r}^{in} = -\sigma_0 (c_T/c_L)^2 \sin 2(\alpha\pi - \theta) \tag{16b}$$

$$\sigma_\theta^{sc}\left(\frac{r}{t}, \theta\right) = \frac{1}{2}(\Sigma_x^L + \Sigma_y^L) - \frac{1}{2}(\Sigma_x^L - \Sigma_y^L) \cos 2\theta - \Sigma_{yx}^L \sin |2\theta| \tag{16c}$$

$$\sigma_{\theta r}^{sc}\left(\frac{r}{t}, \theta\right) = \left[-\frac{1}{2}(\Sigma_x^L - \Sigma_y^L) \sin |2\theta| + \Sigma_{yx}^L \cos 2\theta \right] \operatorname{sgn}(\theta). \tag{16d}$$

In (16c, d)

$$\Sigma_{ij}^L = -\sigma_0[1 - 2(c_T/c_L)^2 \sin^2(\alpha\pi)]\Delta_{ij}^s + \sigma_0 (c_T/c_L)^2 \sin(2\alpha\pi)\Delta_{ij}^a \operatorname{sgn}(\theta) \tag{17}$$

where for $\gamma = a, s$:

$$\Delta_{ij}^\gamma = \int_{r/t}^{c_L} \frac{1}{v^2} \Lambda_{ij}^{1,\gamma}(v, \theta)\, dv + \int_{r/t}^{c_T} \frac{1}{v^2} \Lambda_{ij}^{2,\gamma}(v, \theta)\, dv \tag{18}$$

Also

$$\Lambda_x^{1,s}(v, \theta) = \operatorname{Im}[(s_T^2 - 2\xi_L^2)(s_T^2 - 2s_L^2 + 2\xi_L^2)(s_L^2 - \xi_L^2)^{-1/2} H_L(\xi_L, \bar{c}_L)] \tag{19a}$$

$$\Lambda_y^{1,s}(v, \theta) = \operatorname{Im}[(s_T^2 - 2\xi_L^2)^2 (s_L^2 - \xi_L^2)^{-1/2} H_L(\xi_L, \bar{c}_L)] \tag{19b}$$

$$\Lambda_{yx}^{1,s}(v, \theta) = \operatorname{Im}[-2\xi_L(s_T^2 - 2\xi_L^2) H_L(\xi_L, \bar{c}_L)] \tag{19c}$$

$$\Lambda_x^{1,a}(v, \theta) = \operatorname{Im}[-2\xi_L(s_T^2 - 2s_L^2 + 2\xi_L^2) H_T(\xi_L, \bar{c}_L)] \tag{19d}$$

$$\Lambda_y^{1,a}(v,\theta) = \mathrm{Im}[-2\xi_L(s_T^2 - 2\xi_L^2)H_T(\xi_L, \bar{c}_L)] \tag{19e}$$

$$\Lambda_{yx}^{1,a}(v,\theta) = \mathrm{Im}[4\xi_L^2(s_L^2 - \xi_L^2)^{1/2}H_T(\xi_L, \bar{c}_L)] \tag{19f}$$

$$\Lambda_x^{2,s}(v,\theta) = \mathrm{Im}[-4\xi_T^2(s_T^2 - \xi_T^2)^{1/2}H_L(\xi_T, \bar{c}_L)] \tag{19g}$$

$$\Lambda_y^{2,s}(v,\theta) = \mathrm{Im}[4\xi_T^2(s_T^2 - \xi_T^2)^{1/2}H_L(\xi_T, \bar{c}_L)] \tag{19h}$$

$$\Lambda_{yx}^{2,s}(v,\theta) = \mathrm{Im}[2\xi_T(s_T^2 - 2\xi_T^2)H_L(\xi_T, \bar{c}_L)] \tag{19i}$$

$$\Lambda_x^{2,a}(v,\theta) = \mathrm{Im}[-2\xi_T(s_T^2 - 2\xi_T^2)H_T(\xi_T, \bar{c}_L)] \tag{19j}$$

$$\Lambda_y^{2,a}(v,\theta) = \mathrm{Im}[2\xi_T(s_T^2 - 2\xi_T^2)H_T(\xi_T, \bar{c}_L)] \tag{19k}$$

$$\Lambda_{yx}^{2,a}(v,\theta) = \mathrm{Im}[(s_T^2 - 2\xi_T^2)^2(s_T^2 - \xi_T^2)^{-1/2}H_T(\xi_T, \bar{c}_L)] \tag{19l}$$

and

$$\xi_L(v,\theta) = -\frac{1}{v}\cos\theta + i\left[\left(\frac{1}{v}\right)^2 - s_L^2\right]^{1/2}\sin|\theta| \tag{20}$$

while $\xi_T(v,\theta)$ is defined by eqn (6).

The function $H_\alpha(\xi, w)$, $\alpha = L, T$ is defined as

$$H_\alpha(\xi,w) = \frac{1}{2\pi(s_T^2 - s_L^2)}\frac{(s_\alpha - \xi)^{1/2}(s_\alpha + 1/w)^{1/2}}{(\xi - 1/w)(\xi - s_R)\Gamma_-(\xi)(s_R + 1/w)\Gamma_-(-1/w)} \cdot \frac{d\xi}{d(1/v)} \tag{21}$$

where

$$\Gamma_-(\xi) = \exp\left\{-\frac{1}{\pi}\int_{s_L}^{s_T}\tan^{-1}\left[\frac{4z^2(z^2 - s_L^2)^{1/2}(s_T^2 - z^2)^{1/2}}{(s_T^2 - 2z^2)^2}\right]\frac{dz}{z - \xi}\right\}. \tag{22}$$

In eqns (19), $\bar{c}_L = c_L/\sin(\alpha\pi)$ is the apparent wave speed along the crack faces of the incident L-waves; s_L, s_T and s_R are the slownesses of longitudinal, transverse and Rayleigh waves, respectively. The branch cuts have been taken along the $\mathrm{Re}(\xi_L)$ axis from $\xi_L \to -\infty$ to $\xi_L = -s_L$ and $\xi_L = s_L$ to $\xi_L \to \infty$.

For the superposition problem, the conditions on the crack faces are:

$$\theta = \pm\pi,\ r > 0: \qquad \sigma_\theta = 0 \tag{24a}$$

$$\sigma_{\theta r} = 0 \tag{24b}$$

$$\theta = \kappa\pi \pm 0,\ 0 < r < c_\beta t: \qquad \sigma_\theta = -\sigma_\theta^{st}(r/t, \kappa\pi) \tag{25a}$$

$$\sigma_{\theta r} = -\sigma_{\theta r}^{st}(r/t, \kappa\pi). \tag{25b}$$

Next, we consider the case that the incident wave is a vertically polarized transverse wave of the form:

$$\sigma_{x'y'}^{in} = \sigma_0 H(\tau_T) \tag{26}$$

where τ_T is defined by eqn (2). For the superposition problem the corresponding conditions

on the crack faces are:

$$\theta = \pm\pi,\ r > 0; \qquad \sigma_\theta = 0 \tag{27a}$$

$$\sigma_{\theta r} = 0 \tag{27b}$$

$$\theta = \kappa\pi \pm 0,\ 0 < r < c_F t: \quad \sigma_\theta = -\sigma_\theta^{st}(r/t, \kappa\pi) \tag{28a}$$

$$\sigma_{\theta r} = -\sigma_{\theta r}^{st}(r/t, \kappa\pi) \tag{28b}$$

where σ_θ^{st} and $\sigma_{\theta r}^{st}$ are defined by (15a, b), but

$$\sigma_\theta^{in}\left(\frac{r}{t}, \theta\right) = \sigma_0 \sin 2(\alpha\pi - \theta) \tag{29a}$$

$$\sigma_{\theta r}^{in}\left(\frac{r}{t}, \theta\right) = \sigma_0 \cos 2(\alpha\pi - \theta) \tag{29b}$$

$$\sigma_\theta^{sc}\left(\frac{r}{t}, \theta\right) = \frac{1}{2}(\Sigma_x^T + \Sigma_y^T) - \frac{1}{2}(\Sigma_x^T - \Sigma_y^T)\cos 2\theta - \Sigma_{yx}^T \sin|2\theta| \tag{29c}$$

$$\sigma_{\theta r}^{sc}\left(\frac{r}{t}, \theta\right) = \left[-\frac{1}{2}(\Sigma_x^T - \Sigma_y^T)\sin|2\theta| + \Sigma_{yx}^T \cos 2\theta\right]\operatorname{sgn}(\theta) \tag{29d}$$

in (29c, d)

$$\Sigma_{ij}^T = -\sigma_0 \sin(2\alpha\pi)\cdot\Delta_{ij}^s - \sigma_0 \cos(2\alpha\pi)\,\Delta_{ij}^a \operatorname{sgn}(\theta). \tag{30}$$

Here Δ_{ij}^γ, $\gamma = s, a$, is defined by eqn (18), except that in (19a–l), the apparent wave speed $\bar{c}_L$ should be replaced by the apparent wave speed $\bar{c}_T = c_T/\sin(\alpha\pi)$. The boundary conditions (7)–(8), (24)–(25) and (27)–(28), together with the relevant governing equations, and the initial condition that the solid is at rest for $t < 0$, define initial–boundary–value problems which are very difficult to solve.

APPROXIMATE SOLUTION FOR MODE-III CRACK KINKING

The Mode-III crack kinking problem has been solved in Ref. [3] by taking advantage of the self-similarity of the particle velocity. A crucial step in the analysis of Ref. [3] is the use of Chaplygin's transformation, which reduces the problem to the solution of Laplace's equation in a semi-infinite strip containing a slit. The Schwarz–Christoffel transformation can then be employed to map the semi-infinite strip on a half-plane, and an analytic function in the half-plane which satisfies appropriate conditions along the real axis, can subsequently be constructed. In Ref. [3] the Mode-III stress intensity factor at the tip of the kinked crack has been computed for angles of incidence varying from normal to grazing incidence, for angles of crack kinking defined by $-0.5 \leq \kappa \leq 0.5$, and for arbitrary subsonic crack tip speeds.

In terms of the superposition problem defined by the boundary conditions (7) and (8), there are two main reasons for differences between the stress intensity factors for a kinked crack and a crack which propagates in its own plane. These are firstly the different loading on the new crack faces, as expressed by eqn (8) for $\kappa \neq 0$ and $\kappa = 0$, respectively, and secondly the wedge geometry of the kinked crack at the original crack tip. The drastic assumption can now be made that the difference in loading on the kinked crack faces has the greater effect, at least as far as the near-tip fields are concerned. This assumption then implies that the stress intensity factor for a kinked crack can be approximated by the stress intensity factor for a crack propagating in its own plane for the following conditions on the crack faces

$$\theta = \pm\pi,\ r > 0: \qquad \sigma_{yz} = -\sigma_{\theta z} = 0 \tag{32}$$

$$\theta = \pm 0,\ 0 < r < c_F t: \qquad \sigma_{yz} = -\sigma_{\theta z}^{st}\left(\frac{x}{t}, \kappa\pi\right). \tag{33}$$

The problem formulated by (32) and (33) together with eqn (9) and the initial condition that the solid is at rest prior to $t = 0$ can be solved rigorously.

Let us consider the case that for a crack propagating in its own plane the new crack faces are subjected to running anti-plane shear loads, i.e.

$$\theta = \pm\pi,\ r > 0: \qquad \sigma_{yz} = 0 \tag{34a}$$

$$\theta = 0\pm,\ 0 < r < c_F t: \qquad \sigma_{yz} = \delta\left(\frac{x}{t} - v\right)H(x)H(t) \tag{34b}$$

where δ is the Dirac delta function. Let the stress intensity factor for this fundamental problem be denoted by $K^G_{III}(v, t)$, i.e. $K^G_{III} = \lim_{x \to c_F t}[2\pi(x - c_F t)]^{1/2}\sigma_{yz}|_{y=0}$. It then follows from superposition considerations that for a crack-face loading of the form $-\sigma^{st}_{\theta z}(x/t, \kappa\pi)$ the stress intensity factor becomes

$$K_{III}(c_F, t) = -\int_0^{c_F} \sigma^{st}_{\theta z}(v, \kappa\pi)K^G_{III}(v, t)\,dv. \tag{35}$$

By the use of eqns (3), (4) and (35) we then find

$$K_{III}(c_F, t) = -\sigma_0 \cos(\alpha\pi - \kappa\pi)I(c_F) - \sigma_0 \cos(\alpha\pi)[\sin|\kappa\pi|I_{xz} - \cos(\kappa\pi)I_{yz}] \tag{36a}$$

where

$$I(c_F) = \int_0^{c_F} K^G_{III}(v, t)\,dv \tag{36b}$$

$$I_{iz} = \int_0^{c_F} K^G_{III}(v, t)\left[\int_v^{c_T} \frac{\Lambda_{iz}(v', \kappa\pi)}{(v')^2}\,dv'\right]dv. \tag{36c}$$

In eqn (36c), $i = x$ and $i = y$. The integral given by (36b) is the stress intensity factor for new crack faces, defined by $0 \le x < c_F t$, loaded by uniform anti-plane shear stresses of unit magnitude. The corresponding stress intensity factor can be solved independently and we find $I(c_F) = A(c_F)$, where

$$A(c) = -2\left(\frac{2}{\pi}\right)^{1/2}\left[\frac{c(c_T - c_F)}{c_T(c_T + c - c_F)}\right]^{1/2}(c_T t)^{1/2}. \tag{37}$$

In fact, $A(c)$ as defined by (37) is the stress intensity factor for new crack faces $0 \le x < c_F t$ which are loaded uniformly over $(c_F - c)t \le x < c_F t$.

The evaluation of I_{xz} and I_{yz} has to proceed with caution. Since near-tip stress fields are singular the integration over v contains a square root singularity at $v = 0$. This implies that the integrand in the inner integration over v' is singular as $(v')^{-3/2}$ as $v' \to 0$. Before numerical integration, we have to reduce the order of the singularities. This can be done by changing the order of integration, and evaluating the new inner integrals. We find

$$I_{iz} = \int_0^{c_F} \frac{\Lambda_{iz}(v', \kappa\pi)}{(v')^2}[A(c_F) - A(c_F - v')]\,dv' + A(c_F)$$

$$\times \int_{c_F}^{c_T} \frac{\Lambda_{iz}(v', \kappa\pi)}{(v')^2}\,dv'. \tag{38}$$

Although $\Lambda_{iz}(v', \kappa\pi)\,(v')^{-2}$ behaves as $(v')^{-3/2}$ as $v' \to 0$, the term $[A(c_F) - A(c_F - v')]$ goes to zero as $v' \to 0$. Hence the first integral in eqn (38) contains only a square root singularity at the lower limit, and it can be handled very well by a suitable Jacobi–Gaussian type quadrature. For the second integral, the singular point, $v' = 0$, is outside the interval

of integration. Some care still has to be exercised for cases with a small value of c_F, i.e. for cases with the singular point very close to the end-point of integration. By using a change of variable $v'' = 1/v'$, the integrand in the second integral will decay as $(v'')^{-1/2}$ as v'' increases, which can again be handled very well by a suitable Jacobi–Gaussian type quadrature.

The approximate stress-intensity factors given by eqn (36a) can now be compared with the exact values that have been determined in Ref. [3]. For angles of incidence defined by $\alpha = 0$ (normal incidence) and $\alpha = 0.375$, and for several values of the crack-tip speed, the ratio of the approximate and exact elastodynamic Mode-III stress-intensity factors is shown in Fig. 2. The ratio has been plotted versus the parameter κ, which defined the crack kinking angle. It is noted that the error is small for small values of κ. The error increases as κ increases, but it is always less than 10%.

CRACK KINKING INDUCED BY IN-PLANE WAVES

The fields generated by kinking of a semi-infinite crack upon diffraction of a longitudinal stress wave defined by (13), or a vertically polarized transverse stress wave defined by eqn (26), are extremely difficult to analyze. For the associated superposition problems that the conditions on the crack faces are defined by eqns (24), (25) and eqns (27), (28), respectively. Generally these crack propagation problems involve Mixed Mode I–II fracture.

In principle it should be possible to solve in-plane crack kinking problems by taking advantage of the self-similarity of certain field variables. This was attempted in Ref. [9]. Just as for the Mode-III problem, Chaplygin's transformation was employed to reduce the wave eqns (11a) and (12a) to Laplace's equations in strips containing slits. These strips with slits were mapped in two half-planes, and it was attempted to determine analytic functions that satisfy the boundary conditions. Unfortunately, the analytic functions in the two half-planes are coupled by complicated conditions along the real axes. To solve for these functions it was necessary to reduce the coupling conditions to integral equations, which must be solved numerically. So far, it has not been possible to devise an efficiently converging method to obtain numerical results. That being the case it was decided to explore the possibility of a simple approximate method.

For the anti-plane case it was shown that the near-tip field for a kinked crack can be approximated by the field for a crack propagating in its own plane provided that the new crack faces are subjected to approximate surface tractions. We now follow the same approach for the in-plane problems.

For an incident longitudinal wave the appropriate boundary conditions for the

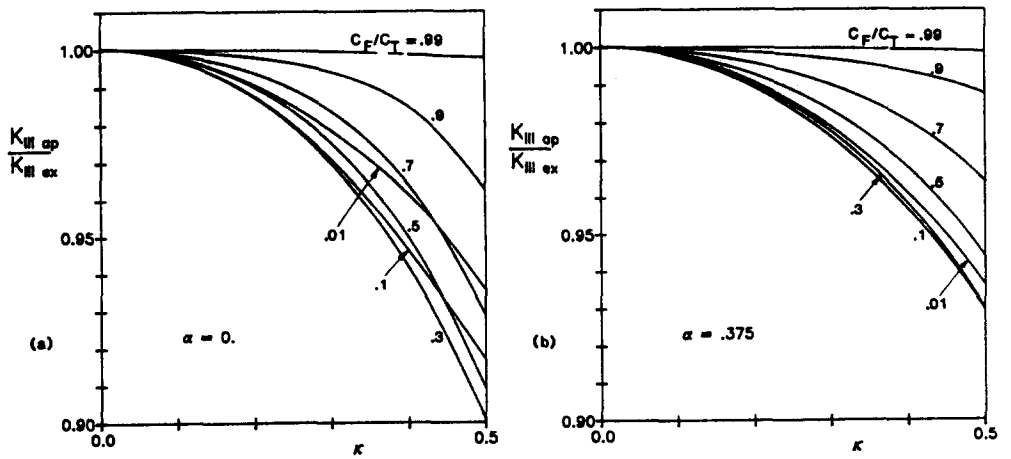

Fig. 2. Ratio of approximate and exact elastodynamic Mode-III stress intensity factors vs κ, for an horizontally polarized transverse wave: (a) $\alpha = 0$, (b) $\alpha = 0.375$.

superposition problem follow from (24) and (25) as

$$\theta = \pm\pi,\ r > 0: \qquad \sigma_y = 0 \tag{39}$$

$$\sigma_{yx} = 0 \tag{40}$$

$$\theta = 0\pm,\ 0 < r < c_F t: \ \sigma_y = -\sigma_\theta^{st}(x/t, \kappa\pi) \tag{41}$$

$$\sigma_{yx} = -\sigma_{r\theta}^{st}(x/t, \kappa\pi). \tag{42}$$

If the stress intensity factors are defined by the limits

$$K_I = \lim_{x \to c_F t} [2\pi(x - c_F t)]^{1/2} \sigma_y|_{y=0} \tag{43}$$

$$K_{II} = \lim_{x \to c_F t} [2\pi(x - c_F t)]^{1/2} \sigma_{yx}|_{y=0} \tag{44}$$

we obtain

$$\frac{K_I^L}{\sigma_0} = -[1 - 2(c_T/c_L)^2 \sin^2(\alpha\pi - \kappa\pi)]E(c_F) - \int_0^{c_F} \frac{[E(c_F) - E(c_F - v)]}{v^2} \times [\Omega_y^{1L}(v) + \Omega_y^{2L}(v)]\,dv - E(c_F)\left[\int_{s_L}^{s_F} \Omega_y^{1L}\left(\frac{1}{v}\right)dv + \int_{s_T}^{s_F} \Omega_y^{2L}\left(\frac{1}{v}\right)dv\right] \tag{45}$$

and

$$\frac{K_{II}^L}{\sigma_0} = (c_T/c_L)^2 \sin 2(\alpha\pi - \kappa\pi)F(c_F) - \int_0^{c_F} \frac{[F(c_F) - F(c_F - v)]}{v^2} \times [\Omega_{yx}^{1L}(v) + \Omega_{yx}^{2L}(v)]\,dv - F(c_F)\left[\int_{s_L}^{s_F} \Omega_{yx}^{1L}\left(\frac{1}{v}\right)dv + \int_{s_T}^{s_F} \Omega_{yx}^{2L}\left(\frac{1}{v}\right)\right]dv \tag{46}$$

where

$$\Omega_y^{mL}(v) = -[1 - 2(c_T/c_L)^2 \sin^2(\alpha\pi)]\bar{\Lambda}_y^{m,s}(v) + (c_T/c_L)^2 \times \sin(2\alpha\pi)\,\mathrm{sgn}(\kappa\pi)\bar{\Lambda}_y^{m,a}(v),\ m = 1, 2 \tag{47}$$

$$\Omega_{yx}^{mL}(v) = -[1 - 2(c_T/c_L)^2 \sin^2(\alpha\pi)]\bar{\Lambda}_{yx}^{m,s}(v) + (c_T/c_L)^2 \sin(2\alpha\pi) \times \mathrm{sgn}(\kappa\pi)\bar{\Lambda}_{yx}^{m,a}(v),\ m = 1, 2 \tag{48}$$

$$\bar{\Lambda}_y^{m,\gamma} = \frac{1}{2}(\Lambda_x^{m,\gamma} + \Lambda_y^{m,\gamma}) - \frac{1}{2}(\Lambda_x^{m,\gamma} - \Lambda_y^{m,\gamma})\cos 2\kappa\pi - \Lambda_{yx}^{m,\gamma} \times \sin|2\kappa\pi|,\ m = 1, 2,\ \gamma = a, s \tag{49}$$

$$\bar{\Lambda}_{yx}^{m,\gamma} = \left[-\frac{1}{2}(\Lambda_x^{m,\gamma} - \Lambda_y^{m,\gamma})\sin|2\kappa\pi| + \Lambda_{yx}^{m,\gamma}\cos 2\kappa\pi\right] \times \mathrm{sgn}(\kappa\pi),\ m = 1, 2,\ \gamma = a, s. \tag{50}$$

Here $E(c)$ and $F(c)$ are the Mode I and Mode II stress intensity factors corresponding to, respectively, unit expanding normal and shear tractions acting from $x = (c_F - c)t$ to $x = c_F t$. These stress intensity factors can be obtained from the work of Nuismer and

Achenbach[10] as

$$\frac{E(c)}{(c_L t)^{1/2}} = -2\left(\frac{2}{\pi}\right)^{1/2} \frac{(c_R - c_F)}{c + c_R - c_F} \frac{1}{S_+(1/c)} \left[\frac{c(c + c_L - c_F)}{c_L(c_L - c_F)}\right]^{1/2}, \tag{51}$$

$$\frac{F(c)}{(c_L t)^{1/2}} = -2\left(\frac{2}{\pi}\right)^{1/2} \frac{(c_R - c_F)}{c + c_R - c_F} \frac{1}{S_+(1/c)} \left[\frac{c(c + c_T - c_F)}{c_L(c_T - c_F)}\right]^{1/2}, \tag{52}$$

where

$$S_+(1/c) = \exp\left[-\frac{1}{\pi}\int_{-s_2}^{-s_4} \frac{1}{z - 1/c} \tan^{-1} \frac{4z^2 |v_L||v_T|}{(v_T^2 - z^2)^2}\, dz\right] \tag{53}$$

$$|v_L| = [(1 - c_F^2/c_L^2)(z + s_2)(z - s_1)]^{1/2}, \tag{54}$$

$$|v_T| = [(1 - c_F^2/c_T^2)(z + s_4)(s_3 - z)]^{1/2}, \tag{55}$$

$$s_1 = \frac{1}{c_L + c_F}, \quad s_2 = \frac{1}{c_L - c_F}, \tag{56a, b}$$

$$s_3 = \frac{1}{c_T + c_F}, \quad s_4 = \frac{1}{c_T - c_F}, \tag{57a, b}$$

The analysis for an incident vertically polarized transverse wave proceeds in a very similar manner. Now the boundary conditions for the superposition problem are

$$\theta = \pm\pi,\ r > 0: \qquad \sigma_y = 0 \tag{58}$$

$$\sigma_{yx} = 0 \tag{59}$$

$$\theta = 0\pm,\ 0 < r < c_F t: \sigma_y = -\sigma_\theta^{sl}(x/t, \kappa\pi) \tag{60}$$

$$\sigma_{yx} = -\sigma_{\theta r}^{sl}(x/t, \kappa\pi). \tag{61}$$

The stress intensity factors are obtained as

$$\frac{K_I^T}{\sigma_0} = -\sin 2(\alpha\pi - k\pi)E(c_F) - \int_0^{c_F} \frac{[E(c_F) - E(c_F - v)]}{v^2}$$
$$\times [\Omega_y^{1T}(v) + \Omega_y^{2T}(v)]\, dv - E(c_F)\left[\int_{s_L}^{s_F} \Omega_y^{1T}\left(\frac{1}{v}\right) dv + \int_{s_T}^{s_F} \Omega_y^{2T}\left(\frac{1}{v}\right) dv\right] \tag{62}$$

$$\frac{K_{II}^T}{\sigma_0} = -\cos 2(\alpha\pi - \kappa\pi)F(c_F) - \int_0^{c_F} \frac{[F(c_F) - F(c_F - v)]}{v^2}$$
$$\times [\Omega_{yx}^{1T}(v) + \Omega_{yx}^{2T}(v)]\, dv - F(c_F)\left[\int_{s_L}^{s_F} \Omega_{yx}^{1T}\left(\frac{1}{v}\right) dv + \int_{s_T}^{s_F} \Omega_{yx}^{2T}\left(\frac{1}{v}\right) dv\right] \tag{63}$$

where

$$\Omega_y^{mT}(v) = -\sin(2\alpha\pi)\bar{\Lambda}_y^{m,s}(v) - \cos(2\alpha\pi)\bar{\Lambda}_y^{m,a}(v)\,\mathrm{sgn}(\kappa\pi),\ m = 1, 2 \tag{64}$$

$$\Omega_{yx}^{mT}(v) = -\sin(2\alpha\pi)\bar{\Lambda}_{yx}^{m,s}(v) - \cos(2\alpha\pi)\bar{\Lambda}_{yx}^{m,a}(v)\,\mathrm{sgn}(\kappa\pi),\ m = 1, 2. \tag{65}$$

Expressions for $\bar{\Lambda}_{ij}^{m,\gamma}$ and $\Lambda_{ij}^{m,\gamma}$, $m = 1, 2$, $\gamma = a, s$, are defined by (49), (50) and (19), except that $\bar{c}_L$ in (19) must be replaced by $\bar{c}_T$.

The Mode I and Mode II stress intensity factors given by eqns (45), (46) and (62), (63) have been computed as functions of κ, for two values of α and for various values of the ratio c_F (crack propagation velocity)/c_R (Rayleigh wave velocity; $\nu = 1/4$). A comparison with the numerical results of Ref. [5] is shown in Tables 1–4, for both incident longitudinal and incident vertically polarized transverse waves. Quite satisfactory agreement may be noted.

Figures 3(a–d) show Mode I and Mode II stress intensity factors for incident longitudinal waves. Corresponding results for incident vertically polarized transverse waves are shown in Figs. 4(a–d). For most cases K_I^L is positive, but K_I^T is positive only for a range of κ roughly defined by $-(1/2)+\alpha < \kappa < \alpha$. A negative Mode I stress intensity factor would correspond to contact of the crack faces near the crack tip. The appearance of a contact zone renders the Mode I stress intensity factor equal to zero, but its effect on the Mode II stress intensity factor may be ignored under the assumption of smooth frictionless crack faces. In the energy considerations of the next section, where use is made of the Mode I and Mode II stress intensity factors, K_I is set identically equal to zero whenever the calculations show it to be negative.

ENERGY CONSIDERATIONS

The approximate elastodynamic stress intensity factors can be used to compute the corresponding energy fluxes into the propagating crack tip. For combined Mode I–II–III fracture, the energy flux into a crack tip may be written in the form[1]:

$$F = -\frac{c_F^3}{2\mu c_T^2 R(c_F)}\{(1-c_F^2/c_L^2)^{1/2}K_I^2 + (1-c_F^2/c_T^2)^{1/2}K_{II}^2\} + \frac{c_F}{2\mu(1-c_F^2/c_T^2)^{1/2}}K_{III}^2, \quad (66)$$

where

$$R(c_F) = (c_F^2/c_T^2 - 2)^2 - 4(1-c_F^2/c_T^2)^{1/2}(1-c_F^2/c_L^2)^{1/2}. \quad (67)$$

The Mode I–II and Mode-III cases will be considered separately.

Table 1. Comparison of numerical values of the stress intensity factors according to Ref. [3]: (1) and this paper: (2), for an incident longitudinal stress wave and $\alpha = 0$

	c_F/c_R	κ	0	.0625	.125	.25	.375	.485
$\frac{K_I^L}{\sigma_0(c_L t)^{1/2}}$	.1	(1)	1.0070	.9870	.9291	.7241	.4625	.2482
		(2)	.9991	.9797	.9234	.7219	.4610	.2829
	.3	(1)	.8484	.8295	.7747	.5818	.3387	.1435
		(2)	.8625	.8435	.7884	.5937	.3481	.1932
	.5	(1)	.7078	.6911	.6427	.4744	.2674	.1068
		(2)	.7023	.6856	.6373	.4695	.2637	.1356
	.7	(1)	.5139	.5011	.4644	.3385	.1895	.0805
		(2)	.5043	.4916	.4549	.3294	.1810	.0899
$\frac{K_{II}^L}{\sigma_0(c_L t)^{1/2}}$	.1	(1)	0.	.1287	.2465	.4131	.4564	.3952
		(2)	0.	.1257	.2410	.4047	.4458	.3848
	.3	(1)	0.	.1342	.2564	.4260	.4636	.3962
		(2)	0.	.1276	.2436	.4023	.4299	.3565
	.5	(1)	0.	.1245	.2373	.3909	.4202	.3551
		(2)	0.	.1197	.2277	.3711	.3887	.3155
	.7	(1)	0.	.1069	.2031	.3301	.3479	.2890
		(2)	0.	.1029	.1951	.3136	.3220	.2570

Table 2. Comparison of numerical values of the stress intensity factors according to Ref. [3]: (1) and this paper: (2), for an incident longitudinal stress wave and $\alpha = 0.375$

	c_F/c_R	κ	0	.0625	.125	.25	.375	.485
$\frac{K_I^L}{\sigma_0(c_L t)^{1/2}}$	.1	(1)	.3761	.4486	.5189	.6277	.6614	.6178
		(2)	.3733	.4466	.5179	.6246	.6424	.5684
	.3	(1)	.3314	.4012	.4763	.6075	.6608	.6197
		(2)	3370	.4100	.4888	.6232	.6658	.5992
	.5	(1)	.2880	.3526	.4257	.5579	.6131	.5702
		(2)	.2859	.3518	.4265	.5600	.6087	.5507
	.7	(1)	.2172	.2684	.3281	.4379	.4834	.4456
		(2)	.2132	.2648	.3249	.4349	.4779	.4344
$\frac{K_{II}^L}{\sigma_0(c_L t)^{1/2}}$	.1	(1)	-.2439	-.2364	-.2104	-.1069	.0375	.1584
		(2)	-.2460	-.2384	-.2096	-.0913	.0764	.2152
	.3	(1)	-.2356	-.2534	-.2461	-.1540	.0092	.1569
		(2)	-.2336	-.2521	-.2430	-.1381	.0481	.2148
	.5	(1)	-.2151	-.2461	-.2491	-.1665	.0013	.1586
		(2)	-.2143	-.2459	-.2475	-.1538	.0333	.2061
	.7	(1)	-.1841	-.2199	-.2281	-.1566	.0006	.1505
		(2)	-.1820	-.2179	-.2250	-.1463	.0227	.1817

Table 3. Comparison of numerical values of the stress intensity factors according to Ref. [3]: (1) and this paper: (2), for an incident transverse stress wave and $\alpha = 0$

	c_F/c_R	κ	0	.0625	.125	.25	.375	.485
$\frac{K_I^T}{\sigma_0(c_L t)^{1/2}}$	.1	(1)	0.	-.3814	-.7365	-1.2803	-1.5241	-1.4983
		(2)	0.	-.3840	-.7397	-1.2693	-1.4607	-1.3524
	.3	(1)	0.	-.3179	-.6086	-1.0231	-1.1571	-1.0589
		(2)	0.	-.3322	-.6347	-1.0558	-1.1560	-1.0130
	.5	(1)	0.	-.2648	-.5021	-.8104	-.8479	-.7102
		(2)	0.	-.2710	-.5133	-.8229	-.8452	-.6830
	.7	(1)	0.	-.1938	-.3622	-.5558	-.5248	-.3790
		(2)	0.	-.1950	-.3656	-.5597	-.5239	-.3699
$\frac{K_{II}^T}{\sigma_0(c_L t)^{1/2}}$	.1	(1)	1.3369	1.2940	1.1695	.7321	.1837	-.2586
		(2)	1.3485	1.3005	1.1610	.6680	.0466	-.5429
	.3	(1)	1.2351	1.1897	1.0590	.6119	.0871	-.2986
		(2)	1.2247	1.1755	1.0339	.5468	-.0295	-.5266
	.5	(1)	1.0823	1.0369	.9070	.4725	-.0095	-.3290
		(2)	1.0784	1.0299	.8910	.4258	-.0906	-.4656
	.7	(1)	.8920	.8493	.7278	.3297	-.0844	-.3199
		(2)	.8817	.8373	.7110	.2972	-.1315	-.3791

Table 4. Comparison of numerical values of the stress intensity factors according to Ref. [3]: (1) and this paper: (2), for an incident transverse stress wave and $\alpha = 0.375$

	c_F/c_R	κ	0	.0625	.125	.25	.375	.485
$\frac{K_I^T}{\sigma_0(c_L t)^{\frac{1}{2}}}$	.1	(1)	.5700	.7357	.8394	.8489	.6495	.4078
		(2)	.5659	.7329	.8375	.8435	.6303	.3677
	.3	(1)	.5166	.6640	.7357	.6391	.3037	-.0401
		(2)	.5253	.6793	.7546	.6560	.3127	-.0303
	.5	(1)	.4591	.5913	.6462	.5108	.1369	-.2282
		(2)	.4557	.5905	.6467	.5104	.1367	-.2179
	.7	(1)	.3526	.4559	.4942	.3653	.0415	-.2621
		(2)	.3462	.4500	.4884	.3590	.0355	-.2630
$\frac{K_{II}^T}{\sigma_0(c_L t)^{\frac{1}{2}}}$	.1	(1)	-.6514	-.4853	-.2901	.1015	.3697	.4402
		(2)	-.6566	-.4902	-.2908	.1153	.3961	.4693
	.3	(1)	-.6471	-.4303	-.1794	.3027	.5820	.5812
		(2)	-.6414	-.4282	-.1790	.2986	.5617	.5333
	.5	(1)	-.6041	-.3750	-.1111	.3931	.6669	.6314
		(2)	-.6018	-.3759	-.1121	.3846	.6322	.5561
	.7	(1)	-.5265	-.3128	-.0634	.4083	.6516	.5947
		(2)	-.5206	-.3100	-.0636	.3968	.6135	.5198

Table 5. Comparison of exact and approximate kinking angle and crack-tip speed for F^*_{max}, with corresponding exact and approximate values of F^*_{max}, for various values of the angle of incidence of a horizontally polarized transverse wave

α		κ	c_F/c_T	F^*_{max}
0.	exact	0.	.62	.765
	appr.	0.	.62	.765
.125	exact	.145	.67	.687
	appr.	.135	.675	.683
.25	exact	.27	.705	.644
	appr.	.265	.715	.633
.375	exact	.395	.735	.610
	appr.	.385	.745	.591
.5	exact	±.5	.76	.570
	appr.	±.5	.78	.545

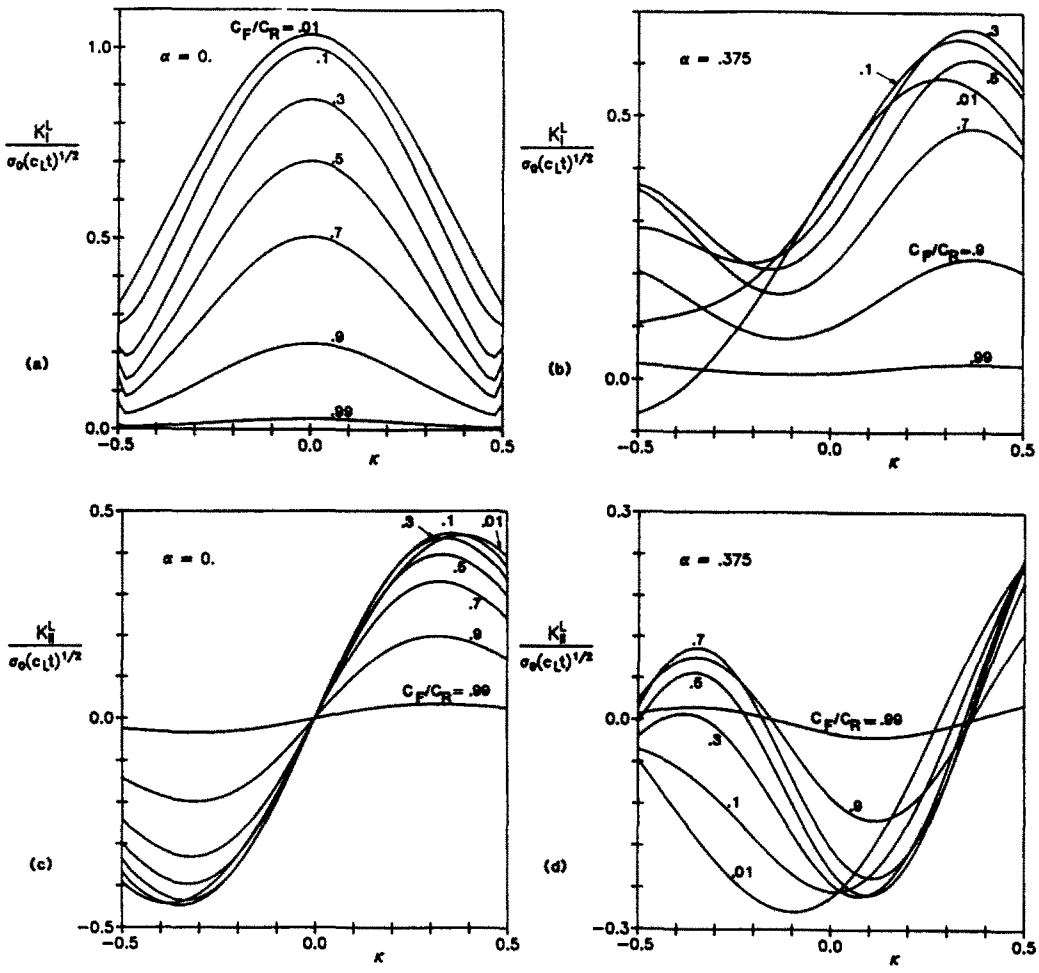

Fig. 3. Elastodynamic stress intensity factors vs κ, $\nu = 0.25$: (a) Mode-I SIF for an incident longitudinal wave, $\alpha = 0$; (b) same as (a) but $\alpha = 0.375$; (c) Mode-II SIF for an incident longitudinal wave, $\alpha = 0$; (d) same as (c) but $\alpha = 0.375$.

Let us define F^* by the relation

$$F = \frac{\sigma_0^2 c_T^2 t}{2\mu} F^*. \tag{68}$$

Since F^* is a quadratic form of the stress intensity factors, the approximation to F^* will not be as good as the one for the stress intensity factors. For the Mode-III case a comparison of approximate and exact results is shown in Fig. 5(a–b) for $\alpha = 0.0$ and $\alpha = 0.375$.

It is of interest to compute the values of c_F and κ at which F^* attains its maximum value with respect to variations of c_F and κ. Results are shown in Tables 5 and 6. The method of this paper appears to yield quite accurate values for κ and c_F at which F^*_{max} will occur. For the Mode III case, the exact and approximate results are compared in Table 5 for several angles of incidence. It is noted that the kinking angle and the crack-tip velocity at which F^* achieves its maximum value, increase as α increases. For an incident L-wave and an incident TV-wave, Tables 6(a, b) list the kinking angle and the crack-tip speed for F^*_{max}, computed on the basis of the approximate results.

CONCLUDING COMMENT

For a crack which has kinked under the influence of an incident stress jump, this paper gives approximate values for the elastodynamic stress intensity factors. The energy criterion suggests that the crack will choose to propagate in the direction and at the

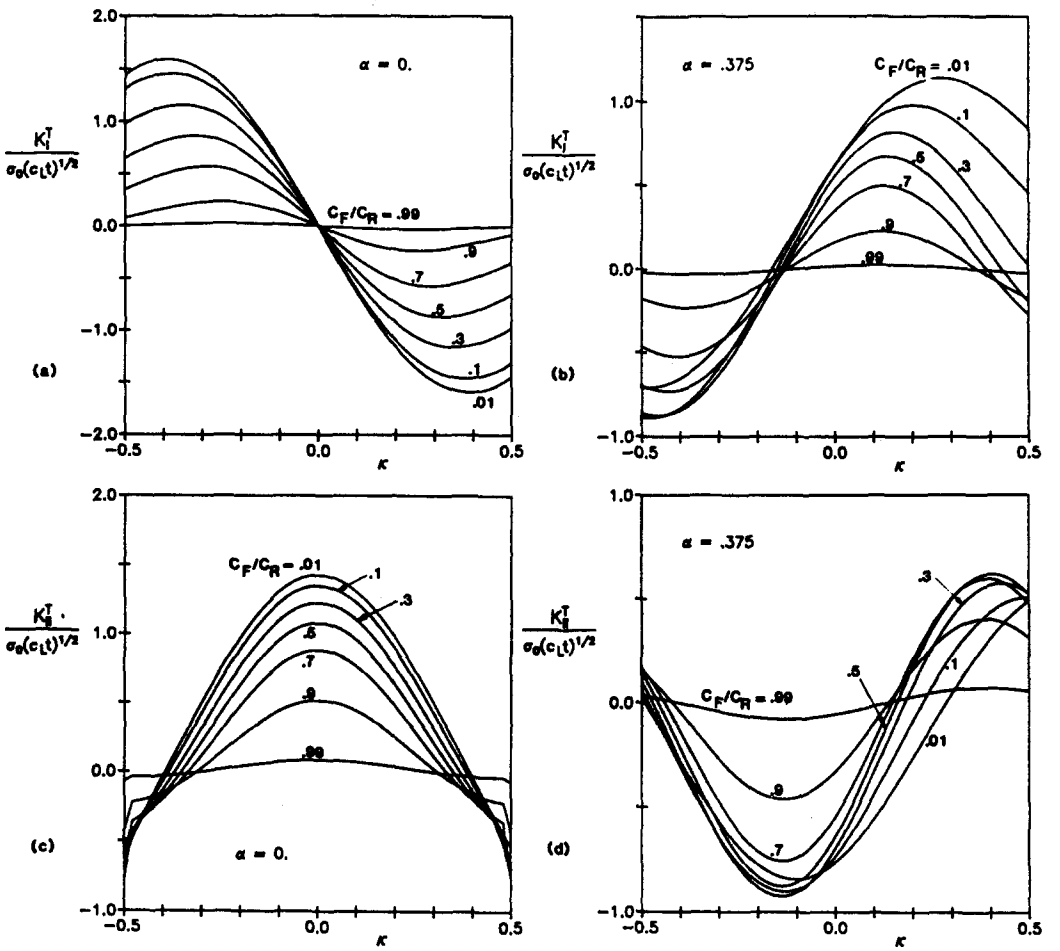

Fig. 4. Elastodynamic stress intensity factors vs κ, $\nu = 0.25$; (a) Mode-I SIF for an incident vertically polarized transverse wave, $\alpha = 0$; (b) same as (a) but $\alpha = 0.375$; (c) Mode-II SIF for an incident vertically polarized transverse wave, $\alpha = 0$; (d) same as (c) but $\alpha = 0.375$.

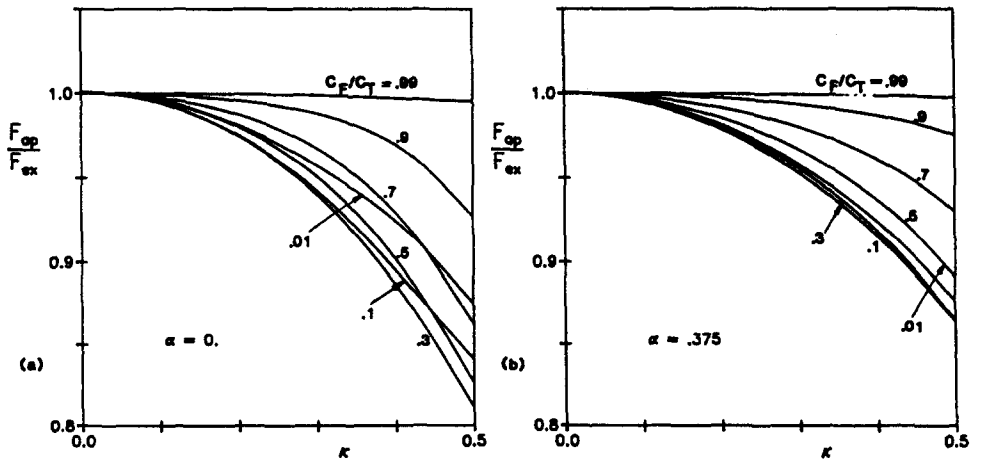

Fig. 5. Ratio of approximate and exact energy fluxes into the crack-tip, plotted vs κ, for an incident horizontally polarized transverse wave: (a) $\alpha = 0$, (b) $\alpha = 0.375$.

Table 6. Kinking angle and crack-tip speed for F^*_{max}, for various angles of incidence of—(a) a longitudinal wave, and (b) a vertically polarized transverse wave

(a)

α	κ	c_F/c_R	F^*_{max}
0.	0.	.56	.358
.125	.120	.585	.344
.25	.25	.615	.326
.375	.38	.67	.301
.5	±.505	.735	.264

(b)

α	κ	c_F/c_R	F^*_{max}
0.	0.	.675	.841
.125	.135	.73	.651
.25	±.265	.77	.539
.375	- 135	.745	.575
.5	0.	.74	.581

velocity for which the energy flux into the crack tip assumes a maximum value. For a number of angles of incidence, Tables 5 and 6 list the values of the kinking angles and the crack-tip speeds at which the flux of energy into the propagating crack tip achieves its maximum value. A rigorous application of the energy criterion would, however, require the elastodynamic stress intensity factors for time-varying kinking angles and crack-tip speeds. These are not available at the present time.

Acknowledgement—This work was carried out in the course of research sponsored by the Air Force Office of Scientific Research under Grant AFOSR 78-3589-E.

REFERENCES

1. J. D. Achenbach, Wave propagation, elastodynamic stress singularities and fracture. In *Theoretical and Applied Mechanics* (Edited by W. T. Koiter), North-Holland, Amsterdam (1976).
2. P. Burgers and J. P. Dempsey, Two analytical solutions for dynamic crack bifurcation in antiplane strain. *J. Appl. Mech.* **49**, 366–370 (1982).
3. J. P. Dempsey, M. K. Kuo and J. D. Achenbach, Mode-III crack kinking under stress-wave loading. *Wave Motion* **4**, 181–190 (1982).
4. P. Burgers, Dynamic propagation of a kinked or bifurcated crack in antiplane strain. *J. Appl. Mech.* **49**, 371–376 (1982).
5. P. Burgers, Dynamic kinking of a crack in plane strain. *Int. J. Solids Structures* **19**, 735–752 (1983).
6. J. D. Achenbach, *Wave Propagation in Elastic Solids*. North-Holland, Amsterdam (1973).
7. J. D. Achenbach, Dynamic effects in brittle fracture. *Mechanics Today* (Edited by S. Nemat-Nasser), Vol. 1, Chap. I, pp. 1–57. Pergamon, New York (1974).
8. L. B. Freund, The analysis of elastodynamic crack tip stress fields. *Mechanics Today* (Edited by S. Nemat-Nasser), Vol. 3, Chap. II, pp. 55–91. Pergamon, New York (1976).
9. J. D. Achenbach and R. P. Khetan, Kinking of a crack under dynamic loading conditions. *J. Elasticity* **9**, 113–129 (1979).
10. R. J. Nuismer, Jr. and J. D. Achenbach, Dynamically induced fracture. *J. Mech. Phys. Solids* **20**, 203–222 (1972).